Singularity Analysis of a Snake Robot and an Articulated Mobile Robot with Unconstrained Links

Motoyasu Tanaka, *Member, IEEE,* and Kazuo Tanaka, *Fellow, IEEE*

***Abstract*—In this paper, we analyze the conditions related to singular configurations with unconstrained links and present related theorems and lemmas for a snake robot and an articulated mobile robot. A snake robot and an articulated mobile robot have the links which have passive or active wheels and the links are serially connected by active joints. The singular configuration should be avoided if the robots are automatically controlled because they cannot execute intended motion when they are in the singular configuration. We derive a novel necessary and sufficient condition for the singular configurations of the snake robot; this removes some limitations of the traditional condition for a snake robot without unconstrained links. We also derive the necessary and sufficient conditions for the singular configurations of the articulated mobile robot, and the structural conditions under which a real articulated mobile robot does not have a singular configuration. These conditions are proved by analyzing the elements of matrices included in kinematic model and considering the geometrical meaning of the elements. In addition, we propose evaluation indices representing the distance from the singular configurations of a snake robot. We verify the effectiveness of these indices through simulations.**

***Index Terms*—Singular configuration, snake robot, articulated mobile robot, unconstrained links, kinematic redundancy**

I. Introduction

SNAKE robots are characterized by the open kinematic chain structure consisting of links serially connected by active joints. They have the mechanism involving anisotropic friction, which means that it is hard to slip sideways, and move by snake-like lateral undulation. One example of the mechanism is the metal edge at the bottom of the links in [1]. The passive wheel is used to add anisotropic friction to the links in many snake robots (e.g., [4]–[8]). Snake robots are useful for in-pipe inspection and search and rescue in disaster areas because they have a slender body and can locomote through the narrow space.

There are two main models for controlling a snake robot. The first model uses the friction of the links and allows the links to slip sideways. This model has been used in control of forward velocity [1], dynamic analysis of three-dimensional motion [2], obstacle-aided locomotion [3], and path-following control of the center of gravity [4]. The second model assumes that the links do not slip sideways [5]–[8]. A controller based on this model can accomplish both trajectory tracking of the robot's head and various tasks using redundancy, as detailed in [6], [7]. We use this latter model in this paper.

M. Tanaka and K. Tanaka are with the Department of Mechanical Engineering and Intelligent Systems, The University of Electro-Communications, Tokyo 182-8585 Japan. (e-mail: mtanaka@uec.ac.jp).

Manuscript received Month Day, 20XX; revised Month Day, 20XX.

The snake robot has singular configurations in which the robot cannot move if the robot is automatically controlled. Prautsch et al. derived the necessary and sufficient condition for singular configurations of the snake robot when all links are wheeled [5]. They used a serpenoid curve [9] as the trajectory of the robot's head to avoid singularities because the snake robot in [5] does not have kinematic redundancy. In contrast, Matsuno et al. introduced an unconstrained link with no wheels into the snake robot to generate kinematic redundancy, and accomplished both trajectory tracking and singularity avoidance using the redundancy as described in [6]. In [7], this control method was applied for a head raising snake robot. A method for switching constrained/unconstrained links by lifting some wheels was proposed in [8]. However, an analysis of singular configurations of the snake robot with unconstrained links has not yet been published. In terms of dynamics, if the snake robot is in the singular configuration, the joint torque for trajectory tracking diverges to infinity as [5]. A real robot is at risk of doing unintended motion because it cannot generate infinite torque, and needs to avoid the unintended motion. In the case of industrial manipulator, it stops or slows down when it is in the region of the neighborhood of singularity as singular protection in ISO10218-1 [10]. The region can be defined by using threshold value and a measure of closeness to singularity, e.g., manipulability [11] and minimum singular value [12]. If the region of the snake robot is appropriately designed, we can plan a safe motion, e.g., stop and slowing down, for the snake robot when the robot is in the neighborhood of the singular configuration. Moreover, the motion for avoiding singularity is needed only into the region, and the robot can use redundancy for other additional tasks, e.g., avoiding falls [7] and an obstacle [8], without trade-off with singularity avoidance at the out of the neighborhood of singular configuration. Thus, it is important to clarify the geometrical condition of singularity and the distance from the singular configurations.

An articulated mobile robot has several segments connected by active joints, and has a powered mechanism generating a propulsion force in the segment (e.g., an active wheel or a crawler). Such a robot is similar to a snake robot, but its motion is not constrained to lateral undulation. There are two well-known methods for controlling articulated mobile robots [13]. The first is the "follow-the-leader" method in which the motion of the head segment is determined and this motion sequentially shifts to the trailing segments, as used in [14]–[17]. The second is the "n-trailer" method in which the robot is steered by treating the motion of the robot as a head segment pulling connected following segments behind it, as used in

[18], [19]. It is difficult to directly change the motion of the other parts of the robot (besides the head) using either of the two methods because the motion of the following segments is determined based on the shift or kinematics that depend on the motion of the head. We have derived the kinematic model of the articulated mobile robot with unconstrained links and the switch of the allocation of unconstrained links. With this extended model, we accomplished following the desired trajectory, avoiding a moving obstacle, and smoothing the input, as demonstrated in [20]. However, as with snake robots, no analysis of singular configurations of the articulated mobile robot with unconstrained links has been published. The geometrical conditions and specific body shapes for singular configurations of a snake or articulated mobile robot with unconstrained links require clarification.

In this paper, we analyze the conditions related to singular configurations with unconstrained links and present related theorems and lemmas for both snake and articulated mobile robots. Furthermore, we propose evaluation indices representing the distance from the singular configuration and conduct simulations to demonstrate their effectiveness. The main contributions of this paper are as follows: 1) We derive a novel necessary and sufficient condition for the singular configurations of the snake robot; this removes some limitations of the traditional condition for a snake robot without unconstrained links as in [5]. 2) We derive the necessary and sufficient conditions for the singular configurations of the articulated mobile robot. 3) We derive the structural conditions under which a real articulated mobile robot does not have a singular configuration. 4) We propose novel evaluation indices for singularities.

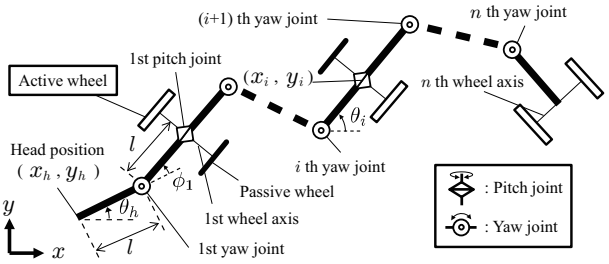

(a) Articulated mobile robot [20] which has some active wheels.

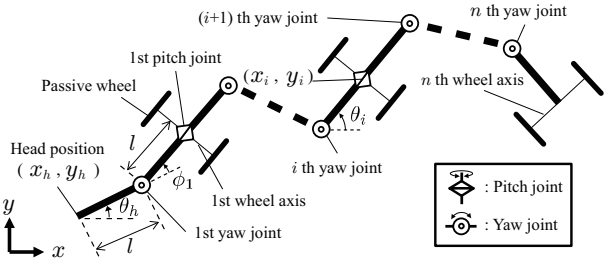

(b) Snake robot which all of the wheels are passive.

Fig. 1. Articulated mobile robot [20] and snake robot.

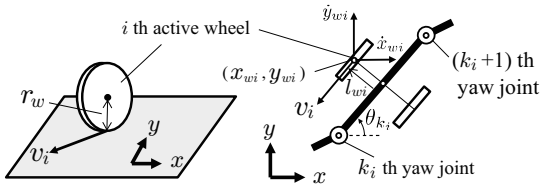

Fig. 2. Position and velocity variables for an active wheel [20].

II. Model and controller

This section describes the kinematic model of an articulated mobile robot (Fig. 1 (a)). The robot and the model are as described in [20]. The robot has n segments, each comprising a pitch rotational joint, a yaw rotational joint, and a pair of wheels. The pitch rotational joint and the pair of wheels are coaxially mounted. All of the joints are active and each wheel is either active or passive. If all of the wheels are passive, the robot is a snake robot in [8] as Fig. 1 (b).

As indicated in Fig. 1, let l be the length of each link, n the number of yaw joints, $\boldsymbol{w} = [x_h, y_h, \theta_h]^T$ the position and attitude of the robot's head, ϕ_i the i-th yaw angle, and (x_i, y_i) the position of the point of intersection of the i-th wheel axis and the link. We set $\boldsymbol{\phi} = [\phi_1, \cdots, \phi_n]^T$, $\theta_i = \theta_h + \sum_{j=1}^{i} \phi_j$ and $\boldsymbol{\theta} = [\theta_h, \boldsymbol{\phi}^T]^T$. We assume that the wheels do not slip sideways. Then, the following equations are satisfied.

$$\dot{x}_i \sin\theta_i - \dot{y}_i \cos\theta_i = 0. \tag{1}$$

The maximum number of active wheels attached to each wheel axis is two. Let $n_w (0 \leq n_w \leq 2n)$ be the total number of active wheels, ρ_i the rotation angle of the i-th active wheel, k_i the index of the wheel axis where the i-th active wheel is attached, (x_{wi}, y_{wi}) the position where the i-th active wheel touches the ground, and r_w the radius of each wheel. We set $\boldsymbol{\rho} = [\rho_1, \cdots, \rho_{n_w}]^T$. We assume that the i-th active wheel does not slip the direction of v_i. From Fig. 2 and considering $v_i = r_w \dot{\rho}_i$, the velocity constraints are obtained as

$$\dot{x}_{wi} \cos\theta_{k_i} + \dot{y}_{wi} \sin\theta_{k_i} + r_w \dot{\rho}_i = 0. \tag{2}$$

Here, we set $\boldsymbol{u} = [\dot{\boldsymbol{\phi}}^T, \dot{\boldsymbol{\rho}}^T]^T$. Considering that (x_i, y_i) and (x_{wi}, y_{wi}) are geometrically represented using $\boldsymbol{w}$ and $\boldsymbol{\phi}$, the following equations are obtained from (1) and (2):

$$\boldsymbol{A}_a(\boldsymbol{\theta})\dot{\boldsymbol{w}} = \boldsymbol{B}_a(\boldsymbol{\theta})\boldsymbol{u}, \tag{3}$$

$$\boldsymbol{A}_b(\boldsymbol{\theta})\dot{\boldsymbol{w}} = \boldsymbol{B}_b(\boldsymbol{\theta})\boldsymbol{u}, \tag{4}$$

where $\boldsymbol{A_a} \in \mathbb{R}^{n\times 3}$, $\boldsymbol{B_a} \in \mathbb{R}^{n\times(n+n_w)}$, $\boldsymbol{A_b} \in \mathbb{R}^{n_w\times 3}$, and $\boldsymbol{B_b} \in \mathbb{R}^{n_w\times(n+n_w)}$. The $1, \cdots, n$-th rows of (3) and $1, \cdots, n_w$-th rows of (4) are equivalent to (1) of $i = 1, \cdots, n$ and (2) of $i = 1, \cdots, n_w$, respectively. Let a_{aij} and a_{bij} be the elements in the i-th row and j-th column of $\boldsymbol{A}_a$ and $\boldsymbol{A}_b$, respectively, and l_{wi} be the length corresponding to the position of the i-th active wheel, as illustrated in Fig. 2. Then

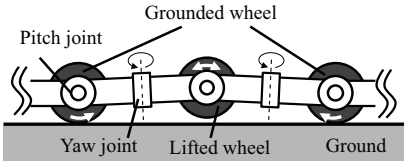

Fig. 3. Pitch joint angles and lifted wheels.

a_{aij} and a_{bij} are obtained as

$$a_{ai1} = \sin\theta_i, \tag{5}$$
$$a_{ai2} = -\cos\theta_i, \tag{6}$$
$$a_{ai3} = -l\{1+\cos(\theta_i-\theta_h)+2\sum_{j=1}^{i-1}\cos(\theta_i-\theta_j)\}, \tag{7}$$
$$a_{bi1} = \cos\theta_{k_i}, \tag{8}$$
$$a_{bi2} = \sin\theta_{k_i}, \tag{9}$$
$$a_{bi3} = -l_{wi}+l\{1+\sin(\theta_{k_i}-\theta_h)+2\sum_{j=1}^{k_i-1}\sin(\theta_{k_i}-\theta_j)\}. \tag{10}$$

When all of the wheels are grounded, the velocity constraint of the robot is represented as

$$\boldsymbol{A}(\boldsymbol{\theta})\dot{\boldsymbol{w}} = \boldsymbol{B}(\boldsymbol{\theta})\boldsymbol{u}, \tag{11}$$

$$\boldsymbol{A}=\begin{bmatrix}A_a\\A_b\end{bmatrix},\ \boldsymbol{B}=\begin{bmatrix}B_a\\B_b\end{bmatrix}=\begin{bmatrix} l & 0 & & \cdots & & 0\\ * & \ddots & \ddots & & & \\ & \ddots & l & 0 & & \vdots\\ \vdots & & * & -r_w & \ddots & \\ & & & \ddots & \ddots & 0\\ * & & \cdots & & * & -r_w\end{bmatrix}, \tag{12}$$

where $\boldsymbol{A} \in \mathbb{R}^{(n+n_w)\times 3}$, $\boldsymbol{B} \in \mathbb{R}^{(n+n_w)\times(n+n_w)}$, and '$*$' signifies nondiagonal elements; their detailed description is omitted. $\boldsymbol{B}$ is always invertible as in (12).

A. Kinematic model with unconstrained links

The snake robot and the articulated mobile robot have kinematic redundancy when unconstrained links are introduced by removing wheels as in [6], [20]. The snake robot can accomplish additional control objectives such as singularity avoidance [6] and fall avoidance [7]. Besides removing the wheels of some links, unconstrained links can be achieved by lifting some wheels as in [8], [20]. The robot in this paper also introduces them by switching the grounded/lifted status of wheels through pitch joint rotation as shown in Fig. 3.

The pitch joints are only used for switching the status of each wheel axis and we assume that the magnitude of the pitch angle is very small and the motion of the pitch joints in the xy-plane does not affect the overall motion of the robot, similar to previous papers [8], [20].

Let σ be the discrete mode number where the i-th wheel axis ($i = n'_1, \cdots, n'_{\bar{n}}$) and j-th active wheel ($j = n'_{w1}, \cdots, n'_{w\bar{a}}$) are grounded. Thus, (11) becomes

$$\boldsymbol{A}_\sigma\dot{\boldsymbol{w}} = \boldsymbol{B}_\sigma\boldsymbol{u}, \tag{13}$$
$$\boldsymbol{A}_\sigma = \begin{bmatrix}\boldsymbol{A}_{a\sigma}\\ \boldsymbol{A}_{b\sigma}\end{bmatrix},\quad \boldsymbol{B}_\sigma = \begin{bmatrix}\boldsymbol{B}_{a\sigma}\\ \boldsymbol{B}_{b\sigma}\end{bmatrix}, \tag{14}$$

where $\boldsymbol{A}_\sigma \in \mathbb{R}^{(\bar{n}+\bar{a})\times 3}$, $\boldsymbol{B}_\sigma \in \mathbb{R}^{(\bar{n}+\bar{a})\times(n+n_w)}$, $\boldsymbol{A}_{a\sigma} \in \mathbb{R}^{\bar{n}\times 3}$, $\boldsymbol{A}_{b\sigma} \in \mathbb{R}^{\bar{a}\times 3}$, $\boldsymbol{B}_{a\sigma} \in \mathbb{R}^{\bar{n}\times(n+n_w)}$, and $\boldsymbol{B}_{b\sigma} \in \mathbb{R}^{\bar{a}\times(n+n_w)}$. $\bar{n}$ and $\bar{a}$ are the number of grounded wheel axes and grounded active wheels in the mode σ, respectively. $\boldsymbol{A}_{a\sigma}$ and $\boldsymbol{B}_{a\sigma}$ denote the matrices for which the i-th row is extracted from $\boldsymbol{A}_a$ and $\boldsymbol{B}_a$, respectively. Similarly, $\boldsymbol{A}_{b\sigma}$ and $\boldsymbol{B}_{b\sigma}$ denote the matrices for which the j-th row is extracted from $\boldsymbol{A}_b$ and $\boldsymbol{B}_b$, respectively.

B. Control input

Similarly to previous papers [8], [20], the joint input is represented as

$$\boldsymbol{u}(t) = \hat{\boldsymbol{u}}_\sigma + \bar{\boldsymbol{u}}_\sigma, \tag{15}$$
$$\hat{\boldsymbol{u}}_\sigma = \boldsymbol{B}_\sigma^\dagger\boldsymbol{A}_\sigma\{\dot{\boldsymbol{w}}_d - \boldsymbol{K}(\boldsymbol{w}-\boldsymbol{w}_d)\}, \tag{16}$$
$$\bar{\boldsymbol{u}}_\sigma = \kappa(\boldsymbol{I}-\boldsymbol{B}_\sigma^\dagger\boldsymbol{B}_\sigma)\boldsymbol{\eta}, \tag{17}$$

where $\boldsymbol{w}_d$ is a desired vector of $\boldsymbol{w}$, $\boldsymbol{K} > \boldsymbol{0}$ is a feedback gain for the main task, $\boldsymbol{B}_\sigma^\dagger$ is a pseudo-inverse matrix of $\boldsymbol{B}_\sigma$, κ is a gain for the sub-task (e.g., singularity avoidance [6] and obstacle avoidance [8]), and $\boldsymbol{\eta} \in \mathbb{R}^{n+n_w}$ is an arbitrary vector and can be designed to accomplish the sub-task as [6], [8], [20]. In (15), $\hat{\boldsymbol{u}}_\sigma$ is an element for the main task and $\bar{\boldsymbol{u}}_\sigma$ is an element representing kinematic redundancy.

By substituting (15) into (13), the closed-loop system is expressed as

$$\boldsymbol{A}_\sigma\{\dot{\boldsymbol{w}} - \dot{\boldsymbol{w}}_d + \boldsymbol{K}(\boldsymbol{w}-\boldsymbol{w}_d)\} = \boldsymbol{0}. \tag{18}$$

Thus, if $\boldsymbol{A}_\sigma$ is of full column rank, $\boldsymbol{w} \to \boldsymbol{w}_d$ is achieved as $t \to \infty$. If $\boldsymbol{A}_\sigma$ is not of full column rank, the convergence of $\boldsymbol{w}$ is not guaranteed because $\dot{\boldsymbol{w}} - \dot{\boldsymbol{w}}_d + \boldsymbol{K}(\boldsymbol{w}-\boldsymbol{w}_d) = \boldsymbol{0}$ does not necessarily hold. This implies that the robot is in a singular configuration, which we shall analyze in the next section. From (18), the size of $\boldsymbol{A}_\sigma$ is also related to whether the controlled variable can be controlled. If $\bar{n} + \bar{a} < 3$, implying that the length of the row is larger than the length of the column in $\boldsymbol{A}_\sigma$, $\boldsymbol{w}$ cannot converge to $\boldsymbol{w}_d$ because $\boldsymbol{A}_\sigma$ is not of full column rank. Thus, it is necessary to satisfy the inequality

$$(\bar{n} + \bar{a}) \geq 3. \tag{19}$$

This means that the number of rows of $\boldsymbol{A}_\sigma$ is larger than or equal to that of columns of $\boldsymbol{A}_\sigma$. Physically, the left term of (19) is a sum of the number of grounded wheel axes and grounded active wheels.

III. Singularity analysis

In this section, we analyze the full column rankness of $\boldsymbol{A}_\sigma$ in the closed-loop system (18) and develop a geometrical condition under which the robot is in a singular configuration. In the case of a snake robot in which all wheels touch the

ground, the robot is in the singular configuration if the body shape is a straight-line or circular arc as [5]. If the body shape of the robot is a straight-line and a circular arc, the robot cannot move to the direction which is parallel to the wheels and the direction of the arc. Thus, it is considered that the robot physically cannot track the arbitrary trajectory in the singular configuration. The robot must avoid such singular configurations. An analytically derived condition for the singular configuration is thus important for control and motion planning.

A. Snake robot when all wheels are grounded ($\bar{n} = n$, $\bar{a} = 0$)

Some lemmas related to the singular configuration of a snake robot were derived in [5]. However, they do not apply for the robot in this study because of mechanical and control variable differences, the head link has passive wheels and the control variable does not include θ_h in [5]. Nevertheless, by analyzing $\boldsymbol{A}_a$, the following theorem can be obtained.

Theorem 1: When $n \geq 3$ and $|\phi_i| < \pi$ $(i = 1, \cdots, n)$, matrix $\boldsymbol{A}_a$ is rank deficient if and only if

$$\phi_2 = \phi_3 = \cdots = \phi_n. \tag{20}$$

Proof: The nonsingular matrix $\boldsymbol{G}$ is defined as

$$\boldsymbol{G} \equiv \begin{bmatrix} \cos\theta_1 & \sin\theta_1 & 0 \\ \sin\theta_1 & -\cos\theta_1 & 0 \\ 0 & 0 & 1 \end{bmatrix}. \tag{21}$$

The rank of a matrix does not change when multiplied by any nonsingular matrices. Multiplying $\boldsymbol{A}_a$ by $\boldsymbol{G}$ from the right yields

$$\boldsymbol{A}'_a = \boldsymbol{A}_a \boldsymbol{G} = \begin{bmatrix} 0 & 1 & -l(\cos\phi_1 + 1) \\ \sin\phi_2 & \cos\phi_2 & -l\{\cos(\phi_1+\phi_2) + 2\cos\phi_2 + 1\} \\ \vdots & \vdots & \vdots \\ \sin\sum_{i=2}^{n}\phi_i & \cos\sum_{i=2}^{n}\phi_i & -l\left(\cos\sum_{i=1}^{n}\phi_i + 2\sum_{i=2}^{n}\cos\sum_{j=i}^{n}\phi_j + 1\right) \end{bmatrix}. \tag{22}$$

We determine the rank of $\boldsymbol{A}'_a$ instead of $\boldsymbol{A}_a$.

(Necessity) If the rank of $\boldsymbol{A}'_a$ changes, the determinant of a submatrix composed of three certain rows of $\boldsymbol{A}'_a$ becomes zero. Let $\boldsymbol{A}'_{ak}$ be the matrix comprising the k, $k+1$, and $k+2$-th rows of $\boldsymbol{A}'_a$ $(1 \leq k \leq n-2)$. The following equation is obtained:

$$\det(\boldsymbol{A}'_{ak}) = l\{\sin(\phi_{k+1} - \phi_{k+2}) + \sin\phi_{k+1} - \sin\phi_{k+2}\}. \tag{23}$$

If $k = 1$, $\phi_2 = \phi_3$ is obtained as a solution when (23) is set to zero. Similarly, by finding the zeros of (23) for $k = 2, \cdots, n-2$, we obtain the necessary condition for $\det(\boldsymbol{A}'_{ak}) = 0$ for all k, that is (20).

(Sufficiency) Sufficiency is demonstrated by substituting (20) into (22). We set $\phi_2 = \phi_3 = \cdots = \phi_n = \alpha$. If $\alpha = 0$, then $\boldsymbol{A}'_a$ becomes

$$\boldsymbol{A}'_a = \begin{bmatrix} 0 & 1 & -l(\cos\phi_1 + 1) \\ \vdots & \vdots & \vdots \\ 0 & 1 & -l(\cos\phi_1 + 2n - 1) \end{bmatrix}. \tag{24}$$

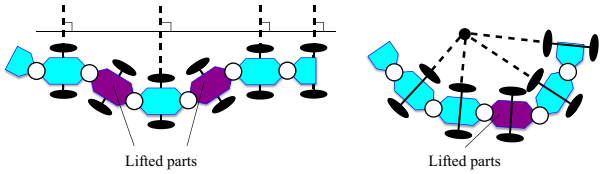

(a) Configuration I: All axes of the grounded wheels are parallel.

(b) Configuration Ⅱ : All extended lines of the axes with grounded wheels intersect at a point.

Fig. 4. Examples of singular configurations for a snake robot.

Hence $\boldsymbol{A}'_a$ is rank deficient because all of the elements of the first column are zero.

If $\alpha \neq 0$, $\boldsymbol{A}'_a$ becomes

$$\boldsymbol{A}'_a = \begin{bmatrix} 0 & 1 & -l(\cos\phi_1 + 1) \\ \sin\alpha & \cos\alpha & -l(\cos(\alpha+\phi_1) + 2\cos\alpha + 1) \\ \vdots & \vdots & \vdots \\ \sin\{(n-1)\alpha\} & \cos\{(n-1)\alpha\} & -l\left(\cos\{(n-1)\alpha+\phi_1\} + 2\sum_{i=1}^{n-1}\cos(i\alpha) + 1\right) \end{bmatrix}. \tag{25}$$

Let $\boldsymbol{c}' \in \mathbb{R}^3$ be defined as follows.

$$\boldsymbol{c}' \equiv \left[\frac{l(\cos\alpha - \sin\alpha\sin\phi_1 + 1)}{\sin\alpha}, \quad l(\cos\phi_1 + 1), \quad 1\right]^T. \tag{26}$$

Then, the column vectors of $\boldsymbol{A}'_a$ are linearly dependent because $\boldsymbol{A}'_a\boldsymbol{c}' = \boldsymbol{0}$. Hence, $\boldsymbol{A}'_a$ is also rank deficient if $\alpha \neq 0$. This proves sufficiency. ■

The rank of $\boldsymbol{A}_a$ only depends on the relative position of the wheel axes and does not depend on θ_h and ϕ_1. Suppose $\phi_2 = \phi_3 = \cdots = \phi_n = \alpha$. If $\alpha = 0$, the body shape of the robot is a straight line; if $\alpha \neq 0$, the body shape of the robot is a circular arc.

B. Snake robot involving axes with lifted wheels ($\bar{n} < n$, $\bar{a} = 0$)

We set $\bar{\theta}_j = \theta_{n'_j} - \theta_{n'_1}$ $(j = 2, \cdots, \bar{n})$. We consider two configurations for a snake robot involving axes with lifted wheels. Configuration I represents a scenario where all grounded wheel axes are parallel, as shown in Fig. 4(a), that is,

$$\sin\bar{\theta}_2 = \sin\bar{\theta}_3 = \cdots = \sin\bar{\theta}_{\bar{n}} = 0. \tag{27}$$

The body shape of the robot in this configuration is more extensive than the previously mentioned straight-line body shape. Configuration Ⅱ represents a scenario where all extended lines of the axes with grounded wheels intersect at a point, as shown in Fig. 4(b). For configuration Ⅱ, the body shape of the robot is more extensive than that for the circular arc. Then, the following theorem is obtained.

Theorem 2: When $\bar{n} \geq 3$, matrix $\boldsymbol{A}_{a\sigma}$ is rank deficient if and only if the robot is in configuration I or Ⅱ.

Proof: The nonsingular matrix $\boldsymbol{G}'$ is defined as

$$\boldsymbol{G}' \equiv \begin{bmatrix} \cos\theta_{n'_1} & \sin\theta_{n'_1} & 0 \\ \sin\theta_{n'_1} & -\cos\theta_{n'_1} & 0 \\ 0 & 0 & 1 \end{bmatrix}. \tag{28}$$

Multiplying $\boldsymbol{A}_{a\sigma}$ by $\boldsymbol{G}'$ from the right results in $\boldsymbol{A}'_{a\sigma}$ as follows:

$$\begin{aligned}\boldsymbol{A}'_{a\sigma}&=\boldsymbol{A}_{a\sigma}\boldsymbol{G}' \\ &=\begin{bmatrix} \boldsymbol{a}'_{a\sigma 1} & \boldsymbol{a}'_{a\sigma 2} & \boldsymbol{a}'_{a\sigma 3} \end{bmatrix} \\ &=\begin{bmatrix} 0 & 1 & -l\left\{1+\cos(\theta_{n'_1}-\theta_h)+2\sum_{k=1}^{n'_1-1}\cos(\theta_{n'_1}-\theta_k)\right\} \\ \sin\bar{\theta}_2 & \cos\bar{\theta}_2 & -l\left\{1+\cos(\theta_{n'_2}-\theta_h)+2\sum_{k=1}^{n'_2-1}\cos(\theta_{n'_2}-\theta_k)\right\} \\ \vdots & \vdots & \vdots \\ \sin\bar{\theta}_{\bar{n}} & \cos\bar{\theta}_{\bar{n}} & -l\left\{1+\cos(\theta_{n'_{\bar{n}}}-\theta_h)+2\sum_{k=1}^{n'_{\bar{n}}-1}\cos(\theta_{n'_{\bar{n}}}-\theta_k)\right\} \end{bmatrix}.\end{aligned} \tag{29}$$

(Necessity) If $\boldsymbol{A}'_{a\sigma}$ is rank deficient, any one of the following cases is satisfied from (29).

Case 1: $\boldsymbol{a}'_{a\sigma 1} = \boldsymbol{0}$.
Case 2: $\boldsymbol{a}'_{a\sigma 2} = \boldsymbol{0}$.
Case 3: $\boldsymbol{a}'_{a\sigma 3} = \boldsymbol{0}$.
Case 4: $\boldsymbol{a}'_{a\sigma 1} \neq \boldsymbol{0}$, $\boldsymbol{a}'_{a\sigma 2} \neq \boldsymbol{0}$, $\boldsymbol{a}'_{a\sigma 3} \neq \boldsymbol{0}$, and there exists $\boldsymbol{c} \neq \boldsymbol{0}$, which satisfies $\boldsymbol{A}'_{a\sigma}\boldsymbol{c} = \boldsymbol{0}$.

(i). If case 1 is satisfied, the robot must satisfy (27) which means configuration I.

(ii). Case 2 cannot be satisfied from the first element of second column of (29).

(iii). We consider case 3. We set the new frame based on the n'_j-th wheel axis as $\Sigma_{n'_j}$ in Fig. 5. With respect to $\Sigma_{n'_j}$, let $({}^{n'_j}x_h, {}^{n'_j}y_h)$ be the position of the robot's head and $({}^{n'_j}x_{n'_j}, {}^{n'_j}y_{n'_j})$ be the position of the intersection point of the n'_j-th wheel axis and the link. From Fig. 5(b), the following relationships are obtained:

$$\begin{aligned}{}^{n'_j}x_{n'_j} &= {}^{n'_j}x_h + l\{1+\cos(\theta_h-\theta_{n'_j}) \\ &\quad + 2\textstyle\sum_{k=1}^{n'_j-1}\cos(\theta_k-\theta_{n'_j})\} = 0 \end{aligned} \tag{30}$$

$$\begin{aligned}{}^{n'_j}y_{n'_j} &= {}^{n'_j}y_h + l\{\sin(\theta_h-\theta_{n'_j}) \\ &\quad + 2\textstyle\sum_{k=1}^{n'_j-1}\sin(\theta_k-\theta_{n'_j})\} = 0 \end{aligned} \tag{31}$$

From (30), $\boldsymbol{a}'_{a\sigma 3}$ in (29) is represented as

$$\boldsymbol{a}'_{a\sigma 3} = \begin{bmatrix} {}^{n'_1}x_h \\ \vdots \\ {}^{n'_{\bar{n}}}x_h \end{bmatrix}. \tag{32}$$

From (32), if $\boldsymbol{a}'_{a\sigma 3} = \boldsymbol{0}$ is satisfied, it is necessary to satisfy ${}^{n'_1}x_h = \cdots = {}^{n'_{\bar{n}}}x_h = 0$. This means that the robot's head is located on all of the extended lines of the grounded wheel axes. Thus, if case 3 is satisfied, it is necessary to satisfy configuration Ⅱ, or all axes with grounded wheels must be located on the same line. The latter geometrical condition is included in configuration I.

(iv). We consider case 4. Let $\boldsymbol{\alpha}_{ai}$ be the i-th row vector of $\boldsymbol{A}'_{a\sigma}$. We focus on the n'_1-th and n'_j-th wheel axes. The rows of $\boldsymbol{A}'_{a\sigma}$ corresponding to these axes are $\boldsymbol{\alpha}_{a1}$ and $\boldsymbol{\alpha}_{aj}$. From (29) and (32), $\tilde{\boldsymbol{A}} = [\boldsymbol{\alpha}_{a1}^T,\ \boldsymbol{\alpha}_{aj}^T]^T$ is expressed as

$$\tilde{\boldsymbol{A}} = \begin{bmatrix} \boldsymbol{\alpha}_{a1} \\ \boldsymbol{\alpha}_{aj} \end{bmatrix} = \begin{bmatrix} 0 & 1 & {}^{n'_1}x_h \\ \sin\bar{\theta}_j & \cos\bar{\theta}_j & {}^{n'_j}x_h \end{bmatrix}. \tag{33}$$

(iv-a). We consider the case of $\sin\bar{\theta}_j = 0$. Then, $\tilde{\boldsymbol{A}}$ is

$$\tilde{\boldsymbol{A}} = \begin{bmatrix} 0 & 1 & {}^{n'_1}x_h \\ 0 & 1 & {}^{n'_j}x_h \end{bmatrix}. \tag{34}$$

Thus, it is necessary to satisfy ${}^{n'_1}x_h = {}^{n'_j}x_h$ if case 4 is satisfied. This means that the n'_1-th and n'_j-th wheel axes are located on the same line. We do not need to consider the case where $\sin\bar{\theta}_j = 0$ is satisfied for all j because this is equivalent to case 1.

(iv-b). We consider the case of $\sin\bar{\theta}_j \neq 0$. Then, the n'_1-th and n'_j-th wheel axes intersect. Let point O be the point where these wheel axes intersect, and r_j be the distance between $(x_{n'_1}, y_{n'_1})$ and point O, as shown in Fig. 5. From Fig. 5, r_j can be expressed as

$$r_j = \frac{l\{1+\cos(\theta_{n'_1}-\theta_{n'_j})+2\sum_{k=n'_1+1}^{n'_j-1}\cos(\theta_k-\theta_{n'_j})\}}{\sin\bar{\theta}_j}. \tag{35}$$

Here, $\boldsymbol{c}_j \in \mathbb{R}^3$ is defined as

$$\boldsymbol{c}_j \equiv \begin{bmatrix} r_j - {}^{n'_1}y_h \\ -{}^{n'_1}x_h \\ 1 \end{bmatrix}. \tag{36}$$

From (30), (31), and (35), we can confirm that $\boldsymbol{\alpha}_{a1}\boldsymbol{c}_j = \boldsymbol{0}$ and $\boldsymbol{\alpha}_{aj}\boldsymbol{c}_j = \boldsymbol{0}$ are satisfied. By focusing on the first element of the first and second columns of (33), we find that $\mathrm{rank}(\tilde{\boldsymbol{A}}) \geq 2$ is satisfied. Then, $\mathrm{rank}(\mathrm{Ker}(\tilde{\boldsymbol{A}})) \leq 1$ holds. Thus, $\boldsymbol{c}_j$ in (36) is the only basis vector of $\tilde{A}$. If $\boldsymbol{c}_2 = \cdots = \boldsymbol{c}_{\bar{n}}$ is satisfied, the following equation must be satisfied.

$$r_2 = \cdots = r_{\bar{n}}. \tag{37}$$

Geometrically, (37) means that all of the extended lines of the axes with grounded wheels intersect at a point. From (iv-a) and (iv-b), it is confirmed that all of the extended lines of the axes with grounded wheels must intersect at a point to satisfy case 4.

(i)–(iv) prove necessity.

(Sufficiency) Next, we confirm the sufficiency of the theorem. If configuration I is satisfied, $\boldsymbol{A}'_{a\sigma}$ is rank deficient because $\boldsymbol{a}_{a\sigma 1} = \boldsymbol{0}$ from (27).

Next, we consider the case when configuration Ⅱ is satisfied. We use $\boldsymbol{c}_j$ in (36). For configuration Ⅱ, r_j is constant and does not depend on the j-th wheel axis, which is used in its calculation, as shown in Fig. 5. Thus,

$$\boldsymbol{c}_2 = \cdots = \boldsymbol{c}_{\bar{n}} = \bar{\boldsymbol{c}}, \tag{38}$$

where $\bar{\boldsymbol{c}} \in \mathbb{R}^3$. Using (35), $\boldsymbol{\alpha}_j\boldsymbol{c}_j = 0$ holds for any j-th wheel axis. Thus, $\boldsymbol{A}'_{a\sigma}$ is rank deficient because $\boldsymbol{A}'_{a\sigma}\bar{\boldsymbol{c}} = \boldsymbol{0}$.

This proves sufficiency. ■

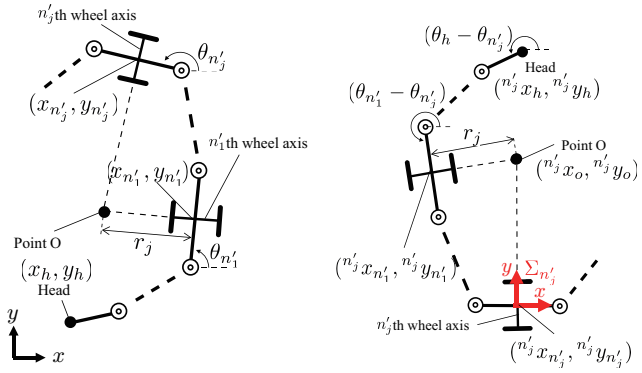

(a) With respect to a fixed frame.

(b) With respect to $\Sigma_{n'_j}$.

Fig. 5. The model of a snake robot with respect to a fixed frame and $\Sigma_{n'_j}$.

C. Articulated mobile robot when all wheels are grounded ($\bar{n} = n$, $\bar{a} > 0$)

In the kinematic model, if axes with ungrounded wheels are considered, the condition describing singular configurations changes because $\boldsymbol{A}_\sigma$ is derived from matrix $\boldsymbol{A}$ with some of its rows removed. With respect to $\boldsymbol{A}$, which refers to active wheels, the following lemma and theorem are obtained.

Lemma 1: When $n_w \geq 1$ and $n + n_w \geq 3$, matrix $\boldsymbol{A}$ is of full column rank if $\phi_2 = \phi_3 = \cdots = \phi_n = 0$.

Proof of this lemma is provided in Appendix A.

Theorem 3: When $n \geq 3$, $n_w \geq 1$, and $|\phi_i| < \pi$ $(i = 2, \cdots, n)$, matrix $\boldsymbol{A}$ is rank deficient if and only if all wheel axes intersect at point O and all active wheels touch the ground at point O.

Proof: Given $\boldsymbol{A}$ and $\boldsymbol{G}$, $\boldsymbol{A}' = \boldsymbol{A}\boldsymbol{G}$ expands as

$$\boldsymbol{A}' = [\boldsymbol{a}'_1 \quad \boldsymbol{a}'_2 \quad \boldsymbol{a}'_3],$$

$$\boldsymbol{a}'_1 = \begin{bmatrix} 0 \\ \sin\phi_2 \\ \vdots \\ \sin\sum_{i=2}^{n}\phi_i \\ \cos(\theta_{k_1} - \theta_1) \\ \vdots \\ \cos(\theta_{k_{n_w}} - \theta_1) \end{bmatrix}, \quad \boldsymbol{a}'_2 = \begin{bmatrix} 1 \\ \cos\phi_2 \\ \vdots \\ \cos\sum_{i=2}^{n}\phi_i \\ -\sin(\theta_{k_1} - \theta_1) \\ \vdots \\ -\sin(\theta_{k_{n_w}} - \theta_1) \end{bmatrix},$$

$$\boldsymbol{a}'_3 = \begin{bmatrix} -l(\cos\phi_1 + 1) \\ -l\{\cos(\phi_1 + \phi_2) + 2\cos\phi_2 + 1\} \\ \vdots \\ -l\left\{\cos\sum_{i=1}^{n}\phi_i + 2\sum_{i=2}^{n}\cos\sum_{j=i}^{n}\phi_j + 1\right\} \\ -l_{w1} + l\{\sin(\theta_{k_1} - \theta_h) + 2\sum_{j=1}^{k_1-1}\sin(\theta_{k_1} - \theta_j)\} \\ \vdots \\ -l_{wn_w} + l\{\sin(\theta_{k_{n_w}} - \theta_h) + 2\sum_{j=1}^{k_{n_w}-1}\sin(\theta_{k_{n_w}} - \theta_j)\} \end{bmatrix}. \quad (39)$$

(Necessity) $\boldsymbol{A}_a$ is formed by the $1, \cdots, n$-th row elements of $\boldsymbol{A}$. From $n \geq 3$ and $n_w \geq 1$, $\boldsymbol{A}_a$ is rank deficient if $\boldsymbol{A}$ is rank deficient. Thus, (20) is satisfied from theorem 1. However, from lemma 1, $\boldsymbol{A}$ has full rank if $\phi_2 = \cdots = \phi_n = 0$. Therefore, if $\boldsymbol{A}$ is rank deficient, it is necessary to satisfy the following equation.

$$\phi_2 = \cdots = \phi_n = \alpha \neq 0 \quad (40)$$

By substituting (40) into (39), the following equations are obtained.

$$\boldsymbol{a}'_1 = \begin{bmatrix} 0 \\ \sin\alpha \\ \vdots \\ \sin\{(n-1)\alpha\} \\ \cos\{(k_1 - 1)\alpha\} \\ \vdots \\ \cos\{(k_{n_w} - 1)\alpha\} \end{bmatrix}, \quad \boldsymbol{a}'_2 = \begin{bmatrix} 1 \\ \cos\alpha \\ \vdots \\ \cos\{(n-1)\alpha\} \\ -\sin\{(k_1 - 1)\alpha\} \\ \vdots \\ -\sin\{(k_{n_w} - 1)\alpha\} \end{bmatrix},$$

$$\boldsymbol{a}'_3 = \begin{bmatrix} -l(\cos\phi_1 + 1) \\ -l(\cos(\alpha + \phi_1) + 2\cos\alpha + 1) \\ \vdots \\ -l(\cos\{(n-1)\alpha + \phi_1\} + 2\sum_{i=1}^{n-1}\cos(i\alpha) + 1) \\ l(\sin\{(k_1 - 1)\alpha + \phi_1\} + 2\sum_{i=1}^{k_1-1}\sin(i\alpha)) - l_{w1} \\ \vdots \\ l(\sin\{(k_{n_w} - 1)\alpha + \phi_1\} + 2\sum_{i=1}^{k_{n_w}-1}\sin(i\alpha)) - l_{wn_w} \end{bmatrix}. \quad (41)$$

From $\alpha \neq 0$, $|\alpha| < \pi$, and (41), the following equation is satisfied.

$$\mathrm{rank}([\boldsymbol{a}'_1 \quad \boldsymbol{a}'_2]) = 2. \quad (42)$$

Thus, if $\boldsymbol{A}'$ is rank deficient, one of following two cases is satisfied.

Case 1: $\boldsymbol{a}'_3 = \boldsymbol{0}$.

Case 2: $\boldsymbol{a}'_3 \neq \boldsymbol{0}$ and there exists a $\boldsymbol{c}' \neq \boldsymbol{0}$ that satisfies $\boldsymbol{A}'\boldsymbol{c}' = \boldsymbol{0}$.

(i). If the first element of $\boldsymbol{a}'_3$ is zero, $\phi_1 = \pi + 2\pi i$ (i is an integer), and then the second element of $\boldsymbol{a}'_3$ is $\cos\alpha + 1 \neq 0$ because of $|\alpha| < \pi$ from (40). Thus, case 1 cannot be satisfied.

(ii). We consider case 2. From (42), we determine that $\mathrm{rank}(\boldsymbol{A}') \geq 2$. Hence, the following inequalities hold:

$$\mathrm{rank}(\mathrm{Ker}(\boldsymbol{A}')) \leq 1, \ \mathrm{rank}(\mathrm{Ker}(\boldsymbol{A})) \leq 1, \quad (43)$$

where $\mathrm{Ker}(\boldsymbol{A})$ is the null space of $\boldsymbol{A}$. If $\boldsymbol{A}$ is not of full column rank, there exists a $\boldsymbol{c}' \in \mathbb{R}^3$ $(\boldsymbol{c}' \neq \boldsymbol{0})$ satisfying $\boldsymbol{A}'\boldsymbol{c}' = \boldsymbol{0}$. Hence, $\boldsymbol{c}'$ is the only basis vector of the null space of $\boldsymbol{A}'$ from (43). Considering the first and second rows of (41), $\boldsymbol{c}'$ is expressed as

$$\boldsymbol{c}' = \left[\frac{l(\cos\alpha - \sin\alpha\sin\phi_1 + 1)}{\sin\alpha}, \ l(\cos\phi_1 + 1), \ 1\right]^T. \quad (44)$$

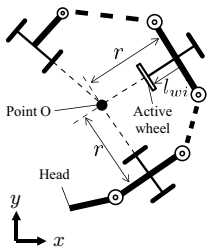

Fig. 6. Point O and r if $\phi_2 = \phi_3 = \cdots = \phi_n = \alpha \neq 0$.

Then, $\boldsymbol{A}'\boldsymbol{c}'$ expands as

$$\boldsymbol{A}'\boldsymbol{c}' = \begin{bmatrix} 0 \\ \vdots \\ 0 \\ r - l_{w1} \\ \vdots \\ r - l_{wn_w} \end{bmatrix}. \tag{45}$$

Here, r is the distance between point O and the position of the intersection point for each wheel axis and the link, as shown in Fig. 6. This is expressed as

$$r = \frac{l(1+\cos\alpha)}{\sin\alpha}. \tag{46}$$

Thus, if $\boldsymbol{A}'\boldsymbol{c}' = \boldsymbol{0}$, then

$$l_{wi} = r \quad (\forall i = 1, \cdots, n_w), \tag{47}$$

holds. The geometrical meaning of (47) is that all of the contact points of the active wheels are located at point O in Fig. 6.

(i) and (ii) prove necessity.

(Sufficiency) If $|\phi_i| < \pi$ $(i = 2, \cdots, n)$ and all wheel axes intersect at a point O, the robot satisfies (40). If all active wheels touch the ground at point O, (47) is satisfied from Fig. 6. By substituting (40) and (47) into (39), $\boldsymbol{A}'\boldsymbol{c}'$ can be obtained as

$$\boldsymbol{A}'\boldsymbol{c}' = \boldsymbol{0}. \tag{48}$$

Thus, $\boldsymbol{A}'$ is rank deficient and sufficiency is proved. ■

Moreover, the following lemma for a real robot is satisfied.

Lemma 2: When $n \geq 3$ and $|\phi_i| < \pi$ $(i = 2, \cdots, n)$, matrix $\boldsymbol{A}$ of a real robot is of full column rank if $n_w \geq 2$.

Proof: From theorem 3, it is necessary to satisfy (47) if $\boldsymbol{A}$ is rank deficient. However, if $n_w \geq 2$, the robot cannot satisfy (47) because the active wheels collide with each other. Thus, $\boldsymbol{A}$ is of full column rank. ■

D. Articulated mobile robot involving axes with lifted wheels ($\bar{n} < n$, $\bar{a} > 0$)

We consider two additional configurations. Configuration Ⅲ represents the case where all of the axes with grounded wheels are on the same line and all active wheels touch the ground at the same point. Configuration Ⅳ represents the case where all of the extended lines of the axes with grounded wheels intersect at a point and all active wheels touch the ground at the intersection point.

Let $p_1, \cdots, p_{\bar{a}}$ be the indices of the axes to which the $n'_{w1}, \cdots, n'_{w\bar{a}}$-th active wheels are attached. Then, the following theorem is obtained.

Theorem 4: Matrix $\boldsymbol{A}_\sigma$ is rank deficient if and only if the robot is in configuration Ⅲ or Ⅳ.

Proof: We set $\tilde{\theta}_j = \theta_{p_j} - \theta_{n'_1}$, $(j = 1, \cdots, \bar{a})$. Multiplying $\boldsymbol{A}_\sigma$ by $\boldsymbol{G}'$ in (28) from the right, $\boldsymbol{A}'_\sigma$ is obtained as

$$\begin{aligned}
\boldsymbol{A}'_\sigma &= \boldsymbol{A}_\sigma \boldsymbol{G}' \\
&= \begin{bmatrix} \boldsymbol{a}'_{\sigma 1} & \boldsymbol{a}'_{\sigma 2} & \boldsymbol{a}'_{\sigma 3} \end{bmatrix}, \\
\boldsymbol{a}'_{\sigma 1} &= \begin{bmatrix} 0 \\ \sin\bar{\theta}_2 \\ \vdots \\ \sin\bar{\theta}_{\bar{n}} \\ \cos\tilde{\theta}_1 \\ \vdots \\ \cos\tilde{\theta}_{\bar{a}} \end{bmatrix}, \ \boldsymbol{a}'_{\sigma 2} = \begin{bmatrix} 1 \\ \cos\bar{\theta}_2 \\ \vdots \\ \cos\bar{\theta}_{\bar{n}} \\ \sin\tilde{\theta}_1 \\ \vdots \\ \sin\tilde{\theta}_{\bar{a}} \end{bmatrix}, \\
\boldsymbol{a}'_{\sigma 3} &= \begin{bmatrix} -l\{1 + \cos(\theta_{n'_1} - \theta_h) + 2\sum_{k=1}^{n'_1 - 1}\cos(\theta_{n'_1} - \theta_k)\} \\ -l\{1 + \cos(\theta_{n'_2} - \theta_h) + 2\sum_{k=1}^{n'_2 - 1}\cos(\theta_{n'_2} - \theta_k)\} \\ \vdots \\ -l\{1 + \cos(\theta_{n'_{\bar{n}}} - \theta_h) + 2\sum_{k=1}^{n'_{\bar{n}} - 1}\cos(\theta_{n'_{\bar{n}}} - \theta_k)\} \\ l\{\sin(\theta_{p_1} - \theta_h) + 2\sum_{k=1}^{p_1 - 1}\sin(\theta_{p_1} - \theta_k)\} - l_{wn'_{w1}} \\ \vdots \\ l\{\sin(\theta_{p_{\bar{a}}} - \theta_h) + 2\sum_{k=1}^{p_{\bar{a}} - 1}\sin(\theta_{p_{\bar{a}}} - \theta_k)\} - l_{wn'_{w\bar{a}}} \end{bmatrix}.
\end{aligned} \tag{49}$$

(Necessity) $\{\tilde{\theta}_1, \cdots, \tilde{\theta}_{\bar{a}}\} \in \{0, \bar{\theta}_2, \cdots, \bar{\theta}_{\bar{n}}\}$ is satisfied because of $\{p_1, \cdots, p_{\bar{a}}\} \in \{n'_1, \cdots, n'_{\bar{n}}\}$. Then, the following equation is satisfied from the first and second column of (49).

$$\mathrm{rank}([\boldsymbol{a}'_{\sigma 1} \quad \boldsymbol{a}'_{\sigma 2}]) = 2. \tag{50}$$

Thus, if $\boldsymbol{A}'_\sigma$ is rank deficient, one of following two cases is satisfied.

Case 1: $\boldsymbol{a}'_{\sigma 3} = \boldsymbol{0}$.

Case 2: $\boldsymbol{a}'_{\sigma 3} \neq \boldsymbol{0}$ and there exists a $\boldsymbol{c} \neq \boldsymbol{0}$ that satisfies $\boldsymbol{A}'_\sigma \boldsymbol{c} = \boldsymbol{0}$.

(i). We consider case 1. From (30) and (31), $\boldsymbol{a}'_{\sigma 3}$ can be represented as

$$\boldsymbol{a}'_{\sigma 3} = \begin{bmatrix} {}^{n'_1}x_h \\ \vdots \\ {}^{n'_{\bar{n}}}x_h \\ {}^{p_1}y_h - l_{wn'_{w1}} \\ \vdots \\ {}^{p_{\bar{a}}}y_h - l_{wn'_{w\bar{a}}} \end{bmatrix}. \tag{51}$$

From a geometrical consideration of (51), ${}^{n'_1}x_h = \cdots = {}^{n'_{\bar{n}}}x_h = 0$ means that all of the axes with grounded wheels and the robot's head must be on the same line. Moreover, ${}^{p_1}y_h - l_{wn'_{w1}} = \cdots = {}^{p_{\bar{a}}}y_h - l_{wn'_{w\bar{a}}} = 0$ means that all of the active wheels have to touch the ground at the position of the robot's head. Thus, if case 1 is satisfied, all of the axes with grounded wheels and the robot's head are on the same line and all active wheels

touch the ground at the position of the robot's head. This geometrical condition is included in configuration Ⅲ.

(ii). We consider case 2. From theorem 2, the robot is in configuration I or Ⅱ if $\bar{n} \geq 3$ and $\boldsymbol{A}_\sigma$ is rank deficient. (ii-a). If the robot is in configuration I, (27) and the following equation are satisfied:

$$\sin\tilde{\theta}_1 = \cdots = \sin\tilde{\theta}_{\bar{a}} = 0. \tag{52}$$

Substituting (27) and (52) into (49), the following equation is obtained.

$$\boldsymbol{A}'_\sigma = \begin{bmatrix} 0 & 1 & {}^{n'_1}x_h \\ \vdots & \vdots & \vdots \\ 0 & 1 & {}^{n'_{\bar{n}}}x_h \\ 1 & 0 & {}^{p_1}y_h - l_{wn'_{w1}} \\ \vdots & \vdots & \vdots \\ 1 & 0 & {}^{p_{\bar{a}}}y_h - l_{wn'_{w\bar{a}}} \end{bmatrix}. \tag{53}$$

Let $\boldsymbol{a}'_k$ be the k-th row vector of (53). The $\boldsymbol{c} \in \mathbb{R}^3$ satisfying $\boldsymbol{a}'_1\boldsymbol{c} = \boldsymbol{0}$ and $\boldsymbol{a}'_{\bar{n}+1}\boldsymbol{c} = \boldsymbol{0}$ can be calculated as

$$\boldsymbol{c} = \begin{bmatrix} {}^{p_1}y_h - l_{wn'_{w1}}, & {}^{n'_1}x_h, & -1 \end{bmatrix}^T. \tag{54}$$

If $\boldsymbol{a}'_k\boldsymbol{c} = \boldsymbol{0}$ is satisfied, the following two equations must be satisfied.

$${}^{n'_1}x_h = \cdots = {}^{n'_{\bar{n}}}x_h, \tag{55}$$

$${}^{p_1}y_h - l_{wn'_{w1}} = \cdots = {}^{p_1}y_h - l_{wn'_{w\bar{a}}}. \tag{56}$$

The geometrical meaning of (55) is that all of the axes with grounded wheels are on the same line, and (56) means that all of the active wheels touch the ground at the same point. Thus, it is necessary to satisfy configuration Ⅲ if $\boldsymbol{A}'_\sigma$ is rank deficient in this case.

(ii-b). If the robot is in configuration Ⅱ, $\bar{\boldsymbol{c}}$ in (38) satisfies $\boldsymbol{A}'_{a\sigma}\bar{\boldsymbol{c}} = \boldsymbol{0}$ as seen in the proof of theorem 2. If $\boldsymbol{A}'_\sigma$ is rank deficient, it is necessary to satisfy $\boldsymbol{A}_{b\sigma}\bar{\boldsymbol{c}} = \boldsymbol{0}$.

We set the new frame based on the p_k-th wheel axis as Σ_{p_k} (see Fig. 7(b)). With respect to Σ_{p_k}, let $({}^{p_k}x_{n'_1}, {}^{p_k}y_{n'_1})$ be the position of intersection point of the n'_1-th wheel axis and the link, and $({}^{p_k}x_o, {}^{p_k}y_o)$ be the position of point O. From Fig. 7(b), the following relationships are obtained:

$$\begin{aligned} {}^{p_k}x_{p_k} =& {}^{p_k}x_{n'_1} + l\{1 + \cos(\theta_{n'_1} - \theta_{p_k}) \\ &+ 2\textstyle\sum_{m=n'_1+1}^{p_k-1}\cos(\theta_m - \theta_{p_k})\} = 0, \end{aligned} \tag{57}$$

$$\begin{aligned} {}^{p_k}y_{p_k} =& {}^{p_k}y_{n'_1} + l\{\sin(\theta_{n'_1} - \theta_{p_k}) \\ &+ 2\textstyle\sum_{m=n'_1+1}^{p_k-1}\sin(\theta_m - \theta_{p_k})\} = 0, \end{aligned} \tag{58}$$

$$\begin{aligned} {}^{p_k}x_o =& {}^{p_k}x_{n'_1} - r_1\sin(\theta_{n'_1} - \theta_{p_k}) = 0, \\ \Rightarrow& {}^{p_k}x_{n'_1} = -r_1\sin\tilde{\theta}_k, \\ {}^{p_k}y_o =& {}^{p_k}y_{n'_1} + r_1\cos\tilde{\theta}_k = r_{p_k}, \\ \Rightarrow& r_{p_k} = r_1\cos\tilde{\theta}_k - l\{\sin(\theta_{n'_1} - \theta_{p_k}) \\ &+ 2\textstyle\sum_{m=n'_1+1}^{p_k-1}\sin(\theta_m - \theta_{p_k})\}. \end{aligned} \tag{59, 60}$$

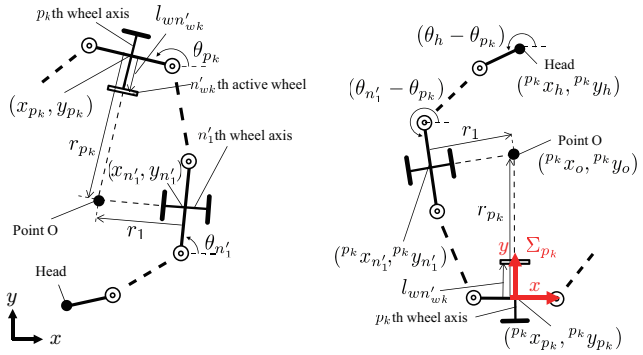

(a) With respect to a fixed frame. (b) With respect to Σ_{p_k}.

Fig. 7. Schematic of the model for configuration Ⅱ.

We focus on $\boldsymbol{a}'_{\bar{n}+k}$, which is formed by the $\bar{n}+k$ $(1 \leq k \leq \bar{a})$-th row vectors of $\boldsymbol{A}'_\sigma$. Corresponding to the $\bar{n}+k$-th row of $\boldsymbol{A}'_\sigma$, $\boldsymbol{a}'_{\bar{n}+k}$ is obtained as

$$\boldsymbol{a}'_{\bar{n}+k} = \begin{bmatrix} \cos\tilde{\theta}_k \\ -\sin\tilde{\theta}_k \\ {}^{p_k}y_h - l_{wn'_{wk}} \end{bmatrix}^T. \tag{61}$$

Considering (60), $\boldsymbol{a}'_{\bar{n}+k}\bar{\boldsymbol{c}}$ is obtained as

$$\boldsymbol{a}'_{\bar{n}+k}\bar{\boldsymbol{c}} = r'_{p_k} - l_{wn'_{wk}}. \tag{62}$$

Thus, to satisfy $\boldsymbol{A}'_\sigma\bar{\boldsymbol{c}} = \boldsymbol{0}$, it is necessary to satisfy the following equation:

$$l_{wn'_{wk}} = r_{p_k} \quad (\forall k = 1, \cdots, \bar{a}). \tag{63}$$

The geometrical meaning of (63) is that all of the active wheels touch the ground at point O. Thus, if $\boldsymbol{A}'_\sigma$ is rank deficient in this case, the robot must be in configuration Ⅳ.

From (i) and (ii), when $\bar{n} \geq 3$, the robot is in configuration Ⅲ or Ⅳ. When $\bar{n} = 1, 2$, the robot is also in configuration Ⅲ or Ⅳ but the detail is omitted. This proves necessity.

(Sufficiency) If the robot is in configuration Ⅲ, (55) and (56) are satisfied. By substituting them into (49) and using $\boldsymbol{c}$ of (54), we can confirm $\boldsymbol{A}'_\sigma\boldsymbol{c} = \boldsymbol{0}$.

If the robot is in configuration Ⅳ, (60) and (63) are satisfied. By substituting them into (49) and using $\bar{\boldsymbol{c}}$ of (38), we can confirm $\boldsymbol{A}'_\sigma\bar{\boldsymbol{c}} = \boldsymbol{0}$.

This proves sufficiency. ■

Lemma 3: Matrix $\boldsymbol{A}_\sigma$ of a real robot is of full column rank if $\bar{a} \geq 2$.

Proof: For a real robot where $\bar{a} \geq 2$, the situations of (56) and (63) do not arise because the active wheels of different wheel axes collide with each other. Thus, (56) and (63) cannot be satisfied. This fact contradicts the assumption that $\boldsymbol{A}_\sigma$ is not of full column rank. That is, $\boldsymbol{A}_\sigma$ of a real robot is of full column rank. ■

From lemma 3, the robot is not in a singular configuration if at least two active wheels touch the ground. This means that the use of redundancy for singularity avoidance is not needed

in this case. However, note that the robot is in a singular configuration corresponding to I or II (see theorem 2) if all of the active wheels are lifted ($\bar{a} = 0$), even if $n_w > 0$. Moreover, if $\bar{a} = 1$, the robot is in a singular configuration corresponding to IV without self-collision.

IV. Evaluation indices of the singular configurations for a snake robot

A snake robot with unconstrained links has two singular configurations, configuration I and II (see theorem 2). The following conventional index is used in [6]–[8] as an evaluation index of the singularities of the snake robot.

$$d_0 \equiv \det(\boldsymbol{A}_{a\sigma}^T \boldsymbol{A}_{a\sigma}). \tag{64}$$

If the robot is in a singular configuration, d_0 becomes 0. Thus, the robot can avoid singularities by increasing d_0. However, the singular configuration that the current body shape approaches if $d_0 \simeq 0$ are not clear from this index. Moreover, the distance between the current body shape and each singular configuration is not evident using this index. This section presents novel indices representing the distance between the current body shape and configuration I or II.

A. Distance from configuration I

We focus on the orientation of the link attached to the k-th wheel axes. Let ψ_k $(k = n'_1, \cdots, n'_{\bar{n}})$ be the orientation of the link with respect to $\Sigma_{n'_1}$ rounding on $[-\pi/2, \pi/2]$. Then, $\psi_{n'_1} = 0$. If the robot is in configuration I, $\psi_{n'_2} = \cdots = \psi_{n'_{\bar{n}}} = 0$ from (27). Thus, if $\psi_{n'_1} = \cdots = \psi_{n'_{\bar{n}}} = 0$, the robot is in configuration I. Then, we define the distance $d_{\rm I}$ from configuration I as

$$d_{\rm I} \equiv \sqrt{\frac{1}{\bar{n}-1} \sum_{k=n'_1}^{n'_{\bar{n}}} (\psi_k - \bar{\psi})^2}, \tag{65}$$

where $\bar{\psi}$ is the mean of ψ_k. (65) is the sample standard deviation of ψ_k and its meaning with respect to distance is straightforward because it is measured in radians. If the robot is in configuration I, $d_{\rm I}$ becomes zero.

B. Distance from configuration II

On the xy plane, the equation of the line representing the k-th wheel axis is

$$x\cos\theta_k + y\sin\theta_k - x_k\cos\theta_k - y_k\sin\theta_k = 0. \tag{66}$$

The signed distance l_k between the point f (x_f, y_f) and the line (66) is obtained as

$$l_k = x_f\cos\theta_k + y_f\sin\theta_k - x_k\cos\theta_k - y_k\sin\theta_k. \tag{67}$$

Let us define $\boldsymbol{L} = [l_{n'_1}, \cdots, l_{n'_{\bar{n}}}]^T$ and $\boldsymbol{w}_f = [x_f, y_f]^T$, $\boldsymbol{L}$ is represented as

$$\boldsymbol{L} = \boldsymbol{C}\boldsymbol{w}_f - \boldsymbol{D}, \tag{68}$$

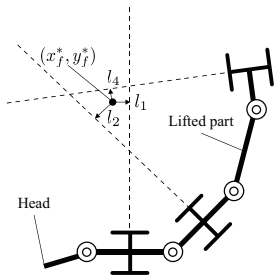

Fig. 8. (x_f^*, y_f^*) and l_k if $n = 4$, $\bar{n} = 3$, $n'_1 = 1$, $n'_2 = 2$, and $n'_3 = 4$.

where

$$\boldsymbol{C} = \begin{bmatrix} \cos\theta_{n'_1} & \sin\theta_{n'_1} \\ \vdots & \vdots \\ \cos\theta_{n'_{\bar{n}}} & \sin\theta_{n'_{\bar{n}}} \end{bmatrix}, \boldsymbol{D} = \begin{bmatrix} x_{n'_1}\cos\theta_{n'_1} + y_{n'_1}\sin\theta_{n'_1} \\ \vdots \\ x_{n'_{\bar{n}}}\cos\theta_{n'_{\bar{n}}} + y_{n'_{\bar{n}}}\sin\theta_{n'_{\bar{n}}} \end{bmatrix}. \tag{69}$$

The solution $\boldsymbol{w}_f^* = [x_f^*, y_f^*]^T$ of (68), which minimizes $||\boldsymbol{L}||$ is obtained as

$$\boldsymbol{w}_f^* = \boldsymbol{C}^{\#}\boldsymbol{D} \tag{70}$$

where $\boldsymbol{C}^{\#}$ is a pseudo inverse matrix of $\boldsymbol{C}$ and is calculated by singular value decomposition (SVD). Fig. 8 shows the geometric relationship of $\boldsymbol{w}_f^*$ because it is the solution of (68) minimizing $||\boldsymbol{L}||$. Then, the distance $d_{\rm II}$ from configuration II is defined as

$$d_{\rm II} \equiv ||\boldsymbol{C}\boldsymbol{w}_f^* - \boldsymbol{D}||. \tag{71}$$

If the robot is in configuration II, $d_{\rm II}$ becomes zero. The distance from configuration II using this value is straightforward to understand because it is the norm of the distance. If the robot is in configuration I, $\mathrm{rank}(\boldsymbol{C}) = 1$. Then, $\boldsymbol{w}_f^*$ becomes the solution minimizing $||\boldsymbol{w}_f^*||$ because the solution is calculated by SVD.

C. Simulations

We validate the effectiveness of the proposed evaluation indices through simulations. We use a snake robot where $n = 4$, $l = 0.05$ [m], $\bar{n} = 3$, and the second wheel axis is lifted. We set $\boldsymbol{w}_h = [0, 0, 0]^T$, $\phi_1 = 0$, and $\phi_2 = \pi/3$, and calculate d_0, $d_{\rm I}$, and $d_{\rm II}$ with ϕ_3 and ϕ_4 varying over $[-3\pi/4, 3\pi/4]$ with a $\pi/240$ interval. Fig. 9 shows the results. d_0 does not allow us to determine whether the shape of the robot is close to either of the singular configurations. In contrast, $d_{\rm I}$ and $d_{\rm II}$ clearly depict the distance from a particular singular configuration.

Fig. 10 (a), (b), and (c) show the indices d_0, $d_{\rm I}$, and $d_{\rm II}$ in the case of $\phi_3 = -\pi/3$, respectively. Fig. 10(c) demonstrates that the robot cannot be in configuration II and Fig. 10(b) shows that it is in configuration I at $\phi_4 = 0$. Fig. 11(a) shows the shape of the robot in this case with the magenta link signifying the lifted part. All of the axes with grounded wheels are parallel in Fig. 11(a). From Fig. 10(c), $d_{\rm II}$ discontinuously changes when the robot is in configuration I ($\phi_4 = 0$). When the robot is in configuration I, $\boldsymbol{C}$ is rank deficient

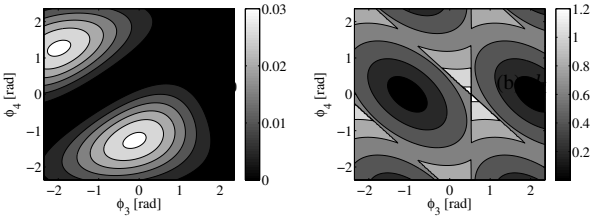

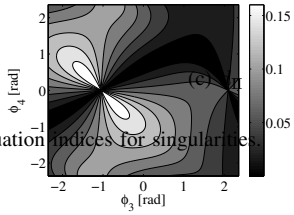

Fig. 9. Evaluation indices for singularities.

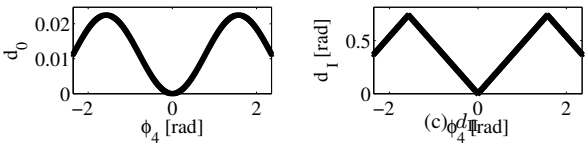

(a) d_0 (b) d_{I}

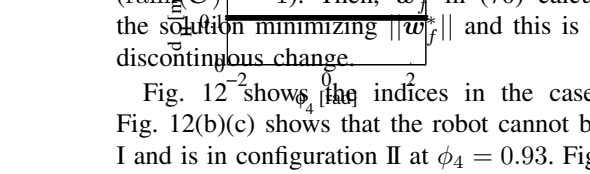

Fig. 10. Evaluation indices for singularities if $\phi_3 = -\pi/3$.

(rank$(\boldsymbol{C}) = 1$). Then, $\boldsymbol{w}_f^*$ in (70) calculated by SVD is the solution minimizing $||\boldsymbol{w}_f^*||$ and this is the reason for the discontinuous change.

Fig. 12 shows the indices in the case of $\phi_3 = \pi/6$. Fig. 12(b)(c) shows that the robot cannot be in configuration I and is in configuration Ⅱ at $\phi_4 = 0.93$. Fig. 11(b) shows the shape of the robot at $\phi_4 = 0.93$ and demonstrates that all of the extended lines of the axes with grounded wheels intersect at a point.

The simulation results confirm that the proposed indices are effective for evaluating the distance from each singular configuration. There is the case where the robot has to stop or slow down to avoid an unintended motion if the robot is in the neighborhood of singular configurations as an industrial manipulator. For example, in an industrial manipulator, the region of neighborhood of singularity is defined and the robot stops or slows down when the robot is in the region. In the snake robot, the distance to each singular configuration is not evident using the conventional index d_0 and it is difficult to set threshold defining the region. In contrast, two proposed indices are straightforward to understand because they are measured in radians and norm of distances, and it is easy to set threshold. Moreover, thresholds for configuration I and Ⅱ can be set separately. These are the merit of using two proposed indices.

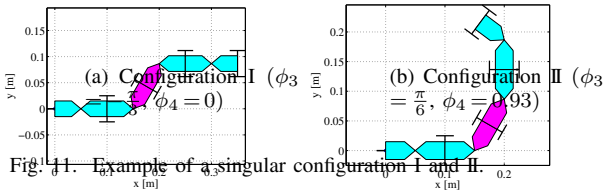

Fig. 11. Example of a singular configuration I and Ⅱ.

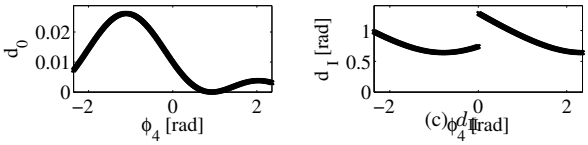

(a) d_0 (b) d_{I}

Fig. 12. Evaluation indices for singularity if $\phi_3 = \pi/6$.

V. Conclusion

In this paper, we analyze the singularity conditions for a snake robot and an articulated mobile robot allowing lifted wheels and present the theorems and lemmas related to the singular configurations. We prove that the singular configurations of the snake robot can correspond only to configurations I and Ⅱ and those of the articulated mobile robot correspond only to configurations Ⅲ and Ⅳ when some wheels are lifted. Additionally, we propose evaluation indices representing the distance from the singular configurations of a snake robot

with unconstrained links, and simulations validate their effectiveness. This paper deals only with singularities on a flat plane, and singularities on complicated terrain (e.g., step [21], cylindrical surface [22]) will comprise our future work.

APPENDIX A
PROOF OF LEMMA 1

Proof: Given $\boldsymbol{A}$ in (12) and $\boldsymbol{G}$ in (21), $\boldsymbol{A}' = \boldsymbol{A}\boldsymbol{G}$ expands as

$$\boldsymbol{A}' = \begin{bmatrix} 0 & 1 & -l(\cos\phi_1 + 1) \\ \vdots & \vdots & \vdots \\ 0 & 1 & -l(\cos\phi_1 + 2n - 1) \\ 1 & 0 & l\sin\phi_1 - l_{w1} \\ \vdots & \vdots & \vdots \\ 1 & 0 & l\sin\phi_1 - l_{wn_w} \end{bmatrix}. \tag{72}$$

The first and second columns are linearly independent in (72).

(i) If $n \geq 2$, focusing on the $1, \cdots, n$-th element of the third column yields that the first and third columns and the second and third columns are both linearly independent. Thus, $\boldsymbol{A}$ is of full column rank if $n \geq 2$.

(ii) If $n = 1$, then $n_w = 2$ must hold to satisfy $n + n_w \geq 3$ and $\det(\boldsymbol{A}')$ is determined as

$$\det(\boldsymbol{A}') = l_{w2} - l_{w1}. \tag{73}$$

$l_{w2} \neq l_{w1}$ is satisfied because the two active wheels are located on the same wheel axis as $n = 1$. Thus, $\boldsymbol{A}$ is of full column rank if $n = 1$.

From (i) and (ii), $\boldsymbol{A}$ is of full column rank. ■

ACKNOWLEDGMENTS

This work was partially supported by JSPS KAKENHI Grant Number 26870198, the Precise Measurement Technology Promotion Foundation, and the ImPACT Program of Council for Science, Technology and Innovation (Cabinet Office, Government of Japan).

REFERENCES

[1] M. Saito, M. Fukaya, and T. Iwasaki, "Serpentine Locomotion with Robotic Snakes," *IEEE Control Systems Magazine*, vol.22, no.1, pp.64-81, 2002.
[2] S. Ma, Y. Ohmameuda, and K. Inoue, "Dynamic Analysis of 3-dimensional Snake Robots," *Proc. IEEE/RSJ Int. Conf. on Intelligent Robots and Systems*, pp.767-772, 2004.
[3] A. Transeth, R. Leine, C. Glocker, K. Pettersen, and P. Liljebäck, "Snake Robot Obstacle-Aided Locomotion: Modeling, Simulations, and Experiments," *IEEE Trans. on Robotics*, vol.24, no.1, pp.88-104, 2008.
[4] P. Liljebäck, I. U. Haugstuen and K. Y. Pettersen, "Path Following Control of Planar Snake Robots Using a Cascaded Approach," *IEEE Trans. on Cont. Sys. Tech*, vol.20, no.1, pp.111-126, 2012.
[5] P. Prautsch, T. Mita, and T. Iwasaki, "Analysis and control of a gait of snake robot," *IEEJ Trans. on Industry Applications*, vol.120, no.3, pp.372-381, 2000.
[6] F. Matsuno and K. Mogi, "Redundancy Controllable System and Control of Snake Robots with Redundancy Based on Kinematic Model," *Proc. IEEE Conf. on Decision and Control*, pp.4791-4796, 2000.
[7] M. Tanaka and F. Matsuno, "Modeling and Control of Head Raising Snake Robots by Using Kinematic Redundancy," *J. of Intelligent and Robotic Systems*, vol.75, no.1, pp.53-69, 2014.
[8] M. Tanaka and F. Matsuno, "Control of Snake Robots with Switching Constraints: trajectory tracking with moving obstacle," *Advanced Robotics*, vol.28, no.6, pp.415-429, 2014.
[9] S. Hirose, Biologically Inspired Robots (Snake-like Locomotor and Manipulator), Oxford University Press, 1993.
[10] ISO 10218-1, "Robots and robotic devices – Safety requirements for industrial robots – Part 1: Robots," 2011.
[11] T. Yoshikawa, "Manipulability of Robotic Mechanisms," *The Int. J. of Robotics Research*, vol.4, no.2, pp.3-9, 1985.
[12] C. A. Klein and B. E. Blaho, "Dexterity Measures for the Design and Control of Kinematically Redundant Manipulators," *The Int. J. of Robotics Research*, vol.6, no.2, pp.72-83, 1987.
[13] G. Granosik, "Hypermobile Robots – the Survey," *J. of Intelligent and Robotic Systems*, vol.75, no.1, pp.147-169, 2014.
[14] S. Hirose, E. F. Fukushima, and S. Tsukagoshi, "Basic Steering Control Methods for The Articulated Body Mobile Robot," *IEEE Control Systems Magazine*, vol.15, no.1, pp.5-14, 1995.
[15] K. L. Paap, F. Kirchner, and B. Klaassen, "Motion Control Scheme for a Snake-Like Robot," *Proc. IEEE Int. Symp. on Computational Intelligence in Robotics and Automation*, pp.59-63, 1999.
[16] M. Kolesnik and H. Streich, "Visual Orientation and Motion Control of MAKRO–Adaptation to the Sewer Environment," *Proc. 7th Int. Conf. on Simulation of Adaptive Behavior on from animals to animats*, pp.62-69, 2002.
[17] H. Yamada and S. Hirose, "Development of Practical 3-Dimensional Active Cord Mechanism ACM-R4," *J. of Robotics and Mechatronics*, vol.18, no.3, pp.305-311, 2006.
[18] T. Kamegawa, T. Yamasaki, H. Igarashi, and F. Matsuno, "Development of the Snake-like Rescue Robot 'KOHGA'," *Proc. IEEE Int. Conf. on Robotics and Automation*, pp.5081-5086, 2004.
[19] B. Murugendran, A. A. Transeth, and S. A. Fjerdingen, "Modeling and Path-following for a Snake Robot with Active Wheels," *IEEE/RSJ Int. Conf. on Intelligent Robots and Systems*, pp.3643-3649, 2009.
[20] M. Tanaka, M. Nakajima, and K. Tanaka, "Smooth Control of an Articulated Mobile Robot with Switching Constraints," *Advanced Robotics*, vol.30, no.1, pp.29-40, 2016.
[21] M. Tanaka and K. Tanaka, "Control of a Snake Robot for Ascending and Descending Steps," *IEEE Transactions on Robotics*, vol.31, no.2, pp.511-520, 2015.
[22] H. Tsukano, M. Tanaka, and F. Matsuno, "Control of a Snake Robot on a Cylindrical Surface Based on a Kinematic Model," *Proc. 9th IFAC Symposium on Robot Control*, pp.865-870, 2009.

Motoyasu Tanaka (S'05 - M'12) received his B.S., M.S., and Ph.D. degrees in Engineering from the Department of Mechanical Engineering and Intelligent Systems at the University of Electro-Communications, Tokyo, Japan, in 2005, 2007, and 2009, respectively. From 2009 to 2012, he worked at Canon, Inc., Tokyo, Japan. He is currently an Assistant Professor in the Department of Mechanical Engineering and Intelligent Systems at the University of Electro-Communications. His research interests include biologically inspired robotics and dynamic-based nonlinear control.

He received the IEEE Robotics and Automation Society Japan Chapter Young Award from the IEEE Robotics and Automation Society Japan Chapter in 2006, and the Best Poster Award at SWARM2015: The First International Symposium on Swarm Behavior and Bio-Inspired Robotics, Kyoto, Japan, in 2015.

He is a member of the Robotics Society of Japan, and the Society of Instrument and Control Engineers.

Kazuo Tanaka (S'87 - M'91 - SM'09 - F'14) received his B.S. and M.S. degrees in Electrical Engineering from Hosei University, Tokyo, Japan, in 1985 and 1987, respectively, and a Ph.D. degree in Systems Science from the Tokyo Institute of Technology, Tokyo, Japan, in 1990. He is currently a Professor in the Department of Mechanical Engineering and Intelligent Systems at the University of Electro-Communications, Tokyo, Japan. He was a visiting computer scientist at the University of North Carolina at Chapel Hill in 1992 and 1993.

He received the Best Young Researcher Award from the Japan Society for Fuzzy Theory and Systems in 1990, the Outstanding Paper Award at the 1990 Annual NAFIPS Meeting in Toronto, Canada, in 1990, the Outstanding Paper Award at the Joint Hungarian-Japanese Symposium on Fuzzy Systems and Applications in Budapest, Hungary, in 1991, the Best Young Researcher Award from the Japan Society for Mechanical Engineering in 1994, the Outstanding Book Award from the Japan Society for Fuzzy Theory and Systems in 1995, 1999 IFAC World Congress Best Poster Paper Prize in 1999, 2000 IEEE Transactions on Fuzzy Systems Outstanding Paper Award in 2000, the Best Paper Selection at 2005 American Control Conference in Portland, USA, in 2005, the Best Paper Award at 2013 IEEE International Conference on Control System, Computing and Engineering (ICCSCE 2013) in Penang, Malaysia, in 2013, and the Best Paper Finalist at 2013 International Conference on Fuzzy Theory and Its Applications (iFUZZY2013) in Taipei, Taiwan, in 2013.

His research interests include intelligent systems and control, nonlinear systems control, robotics, brain–machine interfaces, and their applications. He is currently serving as an Associate Editor for Automatica and for the IEEE Transactions on Fuzzy Systems, and is on the IEEE Control Systems Society Conference Editorial Board.